Insight into the impact of two structural calcium ions on the properties of *Pleurotus eryngii* versatile ligninolytic peroxidase

Yu Gao [a], Lanyan Zheng [a, **], Jian-Jun Li [b, *], Yuguang Du [b, ***]

[a] Department of Microbiology and Parasitology, China Medical University, No.77 Puhe Road, Shenyang 110122, Liaoning Province, China
[b] National Key Laboratory of Biochemical Engineering, National Engineering Research Center for Biotechnology (Beijing), Key Laboratory of Biopharmaceutical Production & Formulation Engineering, PLA, Institute of Process Engineering, Chinese Academy of Sciences, No. 1 North 2nd Street, Beijing 100190, China

A B S T R A C T

Two structural Ca^{2+} (proximal and distal) is known to be important for ligninolytic peroxidases. However, few studies toward impact of residues involved in two Ca^{2+} on properties of ligninolytic peroxidases have been done, especially the proximal one. In this study, mutants of nine residues involved in liganding two Ca^{2+} of *Pleurotus eryngii* versatile peroxidase (VP) were investigated. Most mutants almost completely lost activities, except the mutants of proximal Ca^{2+} - S170A and V192T. In comparison with WT (wild type), optimal pH values of S170A, S170D, and V192T shifted from pH 3.0 to pH 3.5. The order of thermal and pH stabilities of WT, V192T, S170A, and S170D is similar to that of their specific activities: WT > V192T > S170A > S170D. The CD (circular dichroism) results of WT and several mutants indicated that mutations had some effects on secondary structures. For the first time, it was observed that the thermostability of ligninolytic peroxidases is related with proximal Ca^{2+} too, and the mutant containing distal Ca^{2+} only was obtained. Our results clearly demonstrated that enzymatic activities, pH and thermal stabilities, Ca^{2+}content, and secondary structures of VP have close relationship with the residues involved in two structural Ca^{2+}.

© 2016 Elsevier Inc. All rights reserved.

1. Introduction

Rising energy consumption, depletion of fossil fuels and increasing environmental concerns have shifted the focus of energy generation towards biofuels derived from renewable sources. Lignocellulose, as a renewable organic material, consisting of cellulose, hemicellulose and lignin, is the major structural component of plants [1]. Lignin blocks enzymes to access cellulose and hemicellulose. To maximally utilize carbohydrates in the biomass, a pretreatment process is needed to improve accessibility to hydrolytic enzymes. From both economic and environmental perspectives, pretreatment with lignin-degrading microorganisms or enzymes has received renewed interest as an alternative to thermal/chemical pretreatment [2–4].

It's known that several oxidoreductases secreted by white-rot basidiomycetes are involved in lignin biodegradation, including laccase, lignin peroxidase (LiP), manganese peroxidase (MnP), and versatile peroxidase (VP) [1]. Among them, VP is arousing great interest due to its ability to oxidize a variety of substrates [1]. VP has been described in *Pleurotus*, *Bjerkandera* and some other basidiomycetes [5,6]. VP could not only oxidize the substrates that LiP, MnP, and CiP (*Coprinopsis cinerea* peroxidase) can oxidize like veratryl alcohol, Mn^{2+}, and simple phenolic compounds, but also some high-redox-potential aromatic compounds which these three enzymes can't oxidize [1]. A lot of studies towards VP have been carried out, including heterologous overexpression [7,8,9], enzymology [5,8], site-directed mutagenesis [9,10], and protein engineering for improved thermal and H_2O_2 stability [11–14].

VP's crystal structure has been published, contains a heme cofactor located inside an internal cavity, two Ca^{2+} binding regions, and a Mn^{2+} binding site, etc. (Fig. 1) [15]. According to the structure of VP, both calcium ions are coordinated by seven oxygen atoms, which is typical for Ca^{2+}. One calcium ion was reported to be tightly bound on the proximal side of the heme, while the other one was bound on the distal side of heme and considered to be loosely bound

* Corresponding author.
** Corresponding author.
*** Corresponding author.
  E-mail addresses: lyzheng@cmu.edu.cn (L. Zheng), jjli@ipe.ac.cn (J.-J. Li), ygdu@ipe.ac.cn (Y. Du).

[16]. Due to the relative proximity of the calcium ions to the heme, they were proposed to be important for stabilization of the active site of the enzyme. The residues involved in liganding two calcium ions are highly conserved among peroxidases (Fig. 1). It has been found that thermal inactivation of MnP and LiP resulted in loss of distal Ca^2, whereas alkaline treatment of LiP leads to release both Ca^2 [16–19]. Therefore, it appears that the distal Ca^{2+} binding region is related with the thermostability of ligninolytic peroxidases, and both have close relationship with the alkaline stability of ligninolytic peroxidases. Sutherland et al. investigated the role of Asp47 in MnP, one of the ligands of distal Ca^{2+}. They found that the specific activity of D47A was less than 1% of that of WT MnP, and D47A had only one Ca^{2+} and the same spectroscopic properties as thermally inactivated MnP [16]. On the basis of the properties and structure of peanut peroxidase, Reading et al. engineered a disulfide bond near the distal calcium binding site of MnP by mutation of Ala48 and Ala63, and the double mutant MnP A48C/A63C was more stable against the effects of temperature and pH than WT [20]. This study suggested that reinforcing the local structure of the distal Ca^{2+} active site through a disulfide bond would increase enzyme stability.

So far, no systematic studies towards the residues involved in two Ca^{2+} binding pockets of ligninolytic peroxidases have been performed, those liganding the proximal calcium ion in particular. In this study, all residues participating in the two Ca^{2+} binding regions of *Pleurotus eryngii* VP were mutated respectively, and the effects of mutagenesis on specific activity, UV–vis spectroscopy, pH and thermal stability, Ca^{2+} contents, and secondary structure were studied.
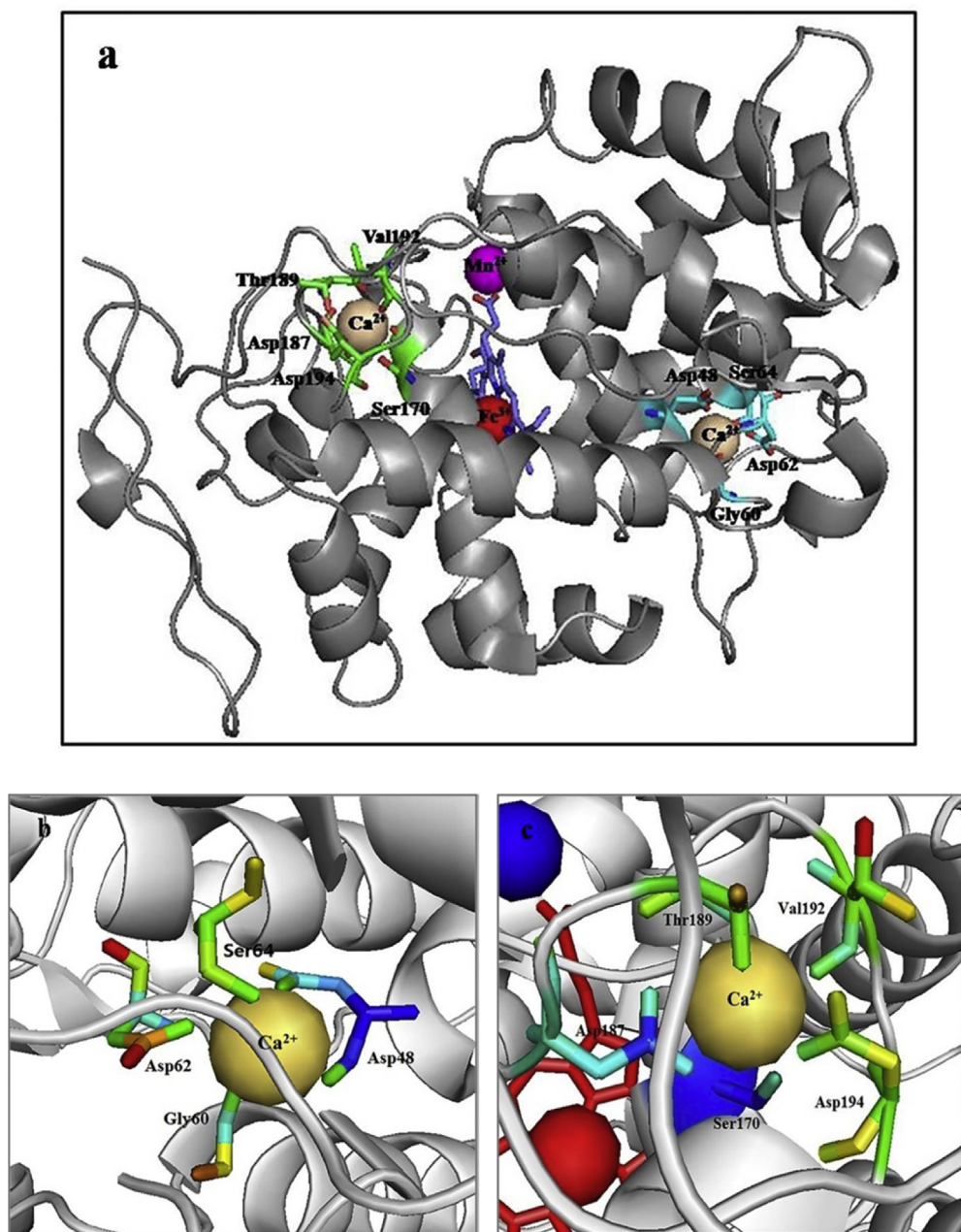
Fig. 1. Crystal structure of VP from *Pleurotus eryngii* (PDB code: 2BOQ) (a) and two "zoom-in" images of the distal (b) and proximal calcium active sites (c). The residues coordinating two structural calcium ions were labelled.

2. Materials and methods

2.1. Materials

Chemicals were from Sigma and Merck. Oligonucleotides were synthesized by Shanghai Sangon Biotech Co. Ltd (China). *Pfu* DNA polymerases from Fermentas. *Dpn*I was from New England BioLabs. The plasmid Mini Kit I was from Omega Bio-tek, and Competent Cell Preparation Kit was from Takara Biotechnology. The nickel column was from Novagen.

2.2. Bacterial strains, plasmids, media and DNA manipulations

E. coli DH5α was used for routine DNA transformation and plasmid isolation. *E. coli* BL21(DE3) was utilized for VP over-expression. *E. coli* strains were routinely grown in Luria-Bertani broth at 37 °C with aeration or on LB supplemented with 1.5% (w/v) agar.

General molecular biology techniques were carried out by standard procedures [21].

2.3. Construction of site-directed mutants, protein overexpression and purification

All site-directed mutants were constructed according to the standard QuikChange Site-Directed Mutagenesis protocol using pET32a-VP as a template and the primers listed in Table S1 (Supporting Information) [8].

WT VP and mutants were overexpressed in *E. coli* BL21(DE3) in the presence of heme under IPTG induction and purified on Nickel column [8]. Proteins were concentrated, and the concentration was determined by the Bradford method using bovine serum albumin as a standard [21].

2.4. Enzyme activity assay

All enzymatic essays against ABTS 2,2′-azinobis (3-ethylbenzothiazoline-6-sulfonate) were done at 200 μl scale in 0.1 M sodium tartrate (pH 3.5) containing 0.1 mM H_2O_2 at 418 nm and 25 °C. The enzymatic activities against Reactive Black 5 (RB5), veratryl alcohol (VA), and Mn^{2+} were carried out following the published procedures [8]. One unit of enzyme activity (U) is defined as the amount of the enzyme that catalyzes conversion of 1 μmol substrate per min. The k_m and v_{max} values for ABTS were determined using Lineweaver-Burk plot. The Rz value equals to A_{407nm}/A_{280nm}.

2.5. UV–vis spectroscopy

UV–visible spectra for all mutants and WT VP were recorded between 250 nm and 550 nm in 10 mM sodium tartrate (pH 5.5) at 25 °C on a multimode reader (Infinite M200 PRO, TECAN).

2.6. Determination of optimal pH and pH stability

The pH-rate profiles were determined using 0.5 mM ABTS in 0.1 M B & R (Britton and Robinson) buffer containing 0.1 mM H_2O_2 over the pH ranges of pH 2.0 to 9.0 at 418 nm and 25 °C.

The pH stability assay was estimated by first preincubating the purified enzymes in B & R buffer at different pH values (pH 2.0 to 8.0) at 4 °C for 1 min, 1 h, 4 h, 25 h, and 120 h respectively. The residual activities were then measured by using 0.5 mM ABTS as the substrate in 0.1 M sodium tartrate (pH 3.5) in the presence of 0.1 mM H_2O_2 at 25 °C immediately. For each enzyme, the highest activity was taken as 100%, and the percentage of the residual activity at different time points and pH values against the highest one was calculated.

2.7. Determination of thermal stability

The thermostabilities of WT and mutants were estimated by measuring the T_{50} values using 96-well gradient thermocyclers (TC-5000, TECHNE), which was defined as the temperature at which the enzyme loses 50% of original activity following incubation for 10 min. After some trials, the enzymes were incubated for 10 min in a gradient temperature ranging from 40 °C to 70 °C for WT VP, 35 °C–65 °C for V192T, 23 °C–53 °C for S170A, and from 25 °C to 55 °C for S170D respectively. After 10 min of incubation, samples were chilled on ice for 10 min and further incubated for 5 min at rt. Afterwards aliquots (50 μl) were subjected to the ABTS-based assay. The thermostability values were deduced from the ratio between the residual activities incubated at different temperature points and the initial activity at rt.

2.8. Determination of calcium concentration in VP

The amount of calcium in the VP samples was determined by inductively coupled plasma optical emission spectrometer (ICP-OES), Thermo Scientific iCAP6300.

The purified enzymes were first dialyzed against 10 mM sodium tartrate (pH 5.5) supplemented with 1 mM $CaCl_2$ and then against 10 mM sodium tartrate (pH 5.5). To remove free Ca^{2+} further, the enzyme samples were again dialyzed against 10 mM sodium tartrate (pH 5.5), which had been treated with Chelex 100 to remove free Ca^{2+} in buffer [22]. The enzyme samples were then loaded onto a Sephadex G-25 column (2.5 × 20 cm), and the column was washed with 10 mM sodium tartrate (pH 5.5) treated with Chelex 100 at a flow rate of 0.4 ml/min. The enzyme solutions were then concentrated with Amicon (10 kDa cut-off) to about 3 ml, and 5 ml of nitric acid (65% w/w) and 2 ml of 30% hydrogen peroxide were added. The vessels were immediately closed after adding the oxidants. The digestion was carried out at 130 °C for 20 min. The digestion products were then concentrated to dryness at 70 °C. Finally, the samples were brought to a volume of 10 ml by adding water.

2.9. Circular dichroism spectroscopy

Far-UV CD spectra (190–260 nm) were recorded for protein samples (0.2 mg/ml) in 50 mM citrate-phosphate buffer (pH 5.5) with a Jasco J-810 spectropolarimeter at 25 °C. Data was averaged over three runs and baselines were subtracted.

Secondary-structure analyses were performed with BeStSel method, which is available at the bestsel.elte.hu server [23]. Secondary structure elements were determined from the PDB (Protein Data Bank) structures using the DSSP (Dictionary of Secondary Structure of Proteins) algorithm for identification. Secondary structures of DSSP include: H, α-helix; G, 3_{10} helix; I, π-helix; E, β-strand; B, β-bridge; S, bend; T, turn; and "others". The components of DSSP, including irregular or loop or residues invisible in the 3D structure, are assigned as "others" [23].

3. Results

3.1. Identification of the target residues for mutagenesis

Based on the crystal structure of *Pleurotus eryngii* VP (PDB code: 2BOQ), the ligands of distal Ca^{2+} include the side chains (carboxylate or hydroxyl) of Asp48, Asp62, and Ser64, the oxygen atoms of the peptide bonds of Gly60 and Asp48, and two water molecules, and those of the proximal one consist of the side chains (hydroxyl

or carboxylate) of Ser170, Asp187, Thr189, Asp194, and the oxygen atoms of the peptide bonds of Ser170, Thr189, and Val192 (Fig. 1). These residues are highly conserved among peroxidases, except variation at the residue 192 (see Supporting Information Fig. S1). All above residues were investigated in this study, and all mutations were confirmed by sequencing.

3.2. Construction, overexpression and purification of site-directed mutants

To investigate the impact of the polar side chains of the residues involved in coordinating two structural calcium ions on enzyme properties, Asp48, Asp62, Ser64, Ser170, Asp187, Thr189, and Asp194 were mutated into Ala with the hydrophobic methyl group, and Ser170 was also mutated into Asp containing the polar side chain for comparison. Gly60 and Val192, which coordinate the calcium ions through the oxygen atoms of the peptide bonds rather than the side chains, were replaced with Ser and Thr containing the polar hydroxyl group respectively. Site-directed mutants were constructed using WT construct pET32a-VP as the template. All mutants were overexpressed in *E. coli* BL21 (DE3), and purified on nickel column (Supporting Information Fig. S2).

3.3. Spectroscopic studies

UV−visible spectra for WT VP, S170D, and S170A were recorded between 250 nm and 700 nm (Fig. 2, Supporting Information Fig. S3), and those for other mutants were scanned between 250 nm and 550 nm (Fig. 2, Supporting Information Fig. S4). No obvious peak was observed around 500 nm (corresponding to CT2 band, charge transfer band) for WT, and three peaks at 536 nm, 564 nm, and 636 nm were seen, which were ascribed to β, α, and CT1 bands respectively (see Supporting Information Fig. S5) [13,15,24]. Similar results were obtained for S170A and S170D (see Supporting Information Figs. S3, S5). An obvious shoulder at around 360 nm was observed in D48A, G60S, S170A, D187A, T189A, and D194A. A slight red shift (around 5 nm) was seen in the Soret band in the mutants D48A, G60S, D62A, S64A, S170D, and V192T. A clear increase at 532 nm was found in D48A, G60S, D62A, and S64A. The Soret peak became wider in D48A, G60S, S170A, D187A, T189A, and D194A due to the appearance of the shoulder at 360 nm.

3.4. Enzymatic activities of wild-type VP and mutants

The specific activities of WT VP and mutants against ABTS are shown in Table 1. Compared with WT, most mutations lead to greatly reduced activities except S170A and V192T, and the specific activities of most mutants lost >98% of that of WT, implying that these amino acids are crucial for VP to maintain activity. The specific activities of S170A and V192T were much higher than the other mutants, and reduced to 23% and 39% of that of WT respectively. Unexpectedly, S170D displayed much lower activity than S170A.

In order to see whether the mutations led to different impact on enzyme activity towards other substrates, the mutants D48A, S170A, D187A, and V192T were chosen to determine their specific activities against RB5, veratryl alcohol (VA), and Mn^{2+} (Table 1). The trends of the variants towards different substrates were similar to that when ABTS was used as the substrate, though the different effects towards different substrates were observed. D48A and D187A showed greatly reduced activity towards RB5, VA, and Mn^{2+}. S170A and V192T exhibited very low activity for RB5 and VA, and retained slightly higher activity against Mn^{2+}.

Most mutants' specific activities were so low that their steady-state kinetics couldn't be measured. Therefore, only the kinetic parameters of WT VP, S170A, S170D, and V192T were determined

(Table 2). Compared with the K_m value of WT, those of S170A and V192T were not affected too much, whereas that of S170D was increased by 3.2-fold. In comparison with WT, the k_{cat} values and the catalytic efficiencies (k_{cat}/K_m) of S170A, S170D, and V192T were significantly reduced, especially the catalytic efficiency of S170D with 182.6-fold decrease.

3.5. pH optima and stabilities of WT VP and mutants

Britton-Robinson buffer (B & R buffer) is a "universal" pH buffer used for the range pH 2 to pH 12, so B & R buffer was chosen for determination of optimal pH and pH stability assay. The pH-activity profiles for WT VP, S170A, S170D, and V192T were determined over the pH ranges 2.0−8.0. The optimal pH of WT VP was at pH 3.0 as reported [11], while that value shifted to 3.5 for three mutants (see Supporting Information Fig. S4). All enzymes showed higher activities over a narrow pH range. As shown in Fig. S3, when pH is above 6.0 or at 2.0, all enzymes nearly completely lost activity except S170D.

The pH stabilities of WT, S170A, S170D, and V192T over the pH ranges 2.0−8.0 were also measured (Fig. 3). At pH 2.0, 8.0, and 9.0, all enzymes were almost completely inactivated after 1 h. Just as reported [11], WT VP remained relatively stable in the pH ranges 3.5−7.0, retaining 70%−90% of initial activity after 120 h. The pH stabilities of four enzymes followed the order of WT > V192T > S170A > S170D, showing a similar trend to the specific activities. S170D, exhibiting the lowest pH stability, completely lost activity over the pH ranges 2.0 to 8.0 after 1 h.

3.6. Thermal stability studies

T_{50} was used to estimate the thermostabilities of WT and S170A, S170D, and V192T (Fig. 4). T_{50} was approximately 59 °C for WT VP, 54 °C for V192T, 44 °C for S170A, and 32 °C for S170D. Therefore, the thermostability followed the order by WT > V192T > S170A > S170D. S170D exhibited the lowest thermostability.

3.7. Determination of calcium concentration in VP

In order to correlate the enzymatic activity of VP with the contents of Ca^{2+}, the calcium concentrations of WT and the representative mutants D48A, S170A, and D187A were determined by ICP-OES (Table 3). The results (in mol Ca^{2+}/mol protein) are as
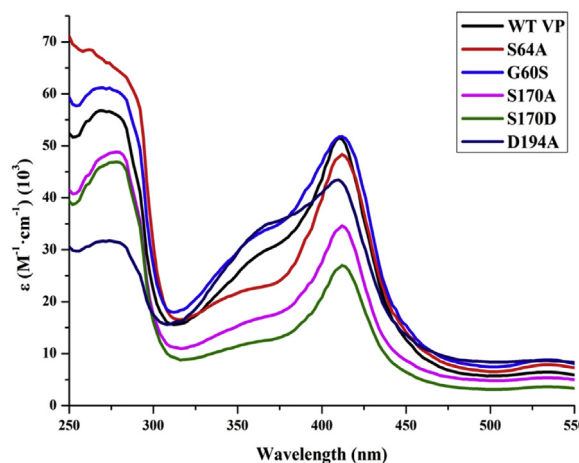
Fig. 2. UV−Vis spectra of wild-type VP and mutants. UV−visible spectra for all mutants and WT VP were scanned between 250 nm and 550 nm in 10 mM sodium tartrate (pH 5.5).

Table 1
The specific activities of WT VP and mutants. Assay conditions are described in Materials and Methods. NA, no activity.

Variants	R_z	Specific activity (%)			
		ABTS	RB5	VA	Mn^{2+}
WT	0.67	100	100	100	100
D48A	0.79	0.04	NA	NA	1.3
G60S	0.84	0.80	NA	NA	NA
D62A	0.89	0.11	NA	NA	NA
S64A	0.73	0.07	NA	NA	NA
S170A	1.16	23.1	4.5	5.7	77.1
S170D	0.73	1.73	NA	NA	NA
D187A	1.09	0.05	NA	NA	6.7
T189A	1.14	0.18	NA	NA	NA
V192T	0.55	39.3	13.6	11.3	28.2
D194A	1.18	0.07	NA	NA	NA

follows: 1.9 for VP WT, 1.5 for S170A, 1.1 for D48A, and 0.7 for D187A.

3.8. Circular dichroism (CD) for WT VP and several mutants

CD was used to investigate the effects of mutations on the conformational or structural changes. Since the tartrate buffer (10 mM, pH 5.5) used for protein storage has a strong background between 190 nm and 250 nm (see Supporting Information Fig. S7), so the tartrate buffer was replaced with the citrate-phosphate buffer (50 mM, pH 5.5). D48A, D187A, S170A, and S170D showed different CD spectra and secondary structures from WT VP, D187A in particular (Fig. 5, Table 4). D48A and S170A exhibited similar secondary structures. The results indicated that mutations had some effects on protein conformation or secondary structure.

4. Discussion

Lignin removal is one of the main limiting factors that lead to high production cost of lignocelluloses-based products. High-redox-potential ligninolytic peroxidases are important for that process. VP, as a type of newly discovered high-redox-potential ligninolytic peroxidase, received great interest due to catalytic promiscuity [1]. The structure-function relationship of VP has been well studied [9,10,12–14]. However, few studies toward the relationship between structure and the thermal/pH stability of VP have been done.

In the current study, we focus on the impact of the residues involved in two Ca^{2+} binding sites of VP on specific activity, UV–vis spectroscopy, the thermal and pH stability, Ca^{2+} concentration, and secondary structure. Ten site-directed mutants of VP were constructed and characterized.

A red shift in the Soret peak from 407 to 412 nm and an obvious absorption peak at 360 nm were seen in some mutants. An increase at 532 nm was found only in the mutants of the residues liganding the distal calcium ion. It appears that mutations of the residues from two Ca^{2+} binding sites had different effects on UV–vis spectroscopy. The shoulder at 360 nm, which has been observed in

Table 2
Kinetic parameters of WT VP and mutants. Assay conditions are described in Materials and Methods, and ABTS was used as the substrate.

	K_m (μM)	k_{cat} (s^{-1})	k_{cat}/K_m (s^{-1} μM^{-1})
WT	1.26 ± 0.1	0.53 ± 0.02	0.42
S170A	1.11 ± 0.07	0.12 ± 0.002	0.11
S170D	3.98 ± 0.47	0.009 ± 0.003	0.0023
V192T	0.85 ± 0.0	0.21 ± 0.005	0.25

many low-spin iron (III) species, coupled with the red shift of the Soret absorbance and the peak at 532 nm in some mutants, suggested that the heme iron had formed a low-spin hexacoordinate complex, as was shown previously for MnP D47A and thermally inactivated MnP and LiP [16,20,24].

Compared with WT VP, the optimal pH values of S170A, S170D, and V192T shifted from pH 3.0 to pH 3.5. The similar shift was also found in some other mutants [11]. However, the pH stabilities of all mutants were significantly dropped. The order of the pH stabilities of WT, V192T, S170A, and S170D is similar to that of their specific activities. Just like pH stability, the order of the thermostabilities of WT, V192T, S170A, and S170D is similar to that of their specific activities. These results confirmed that the pH and thermal stabilities of VP are closely related with the residues liganding proximal Ca^{2+} and the Ca^{2+} contents (Table 3). For the first time, it was observed that the thermostability of ligninolytic peroxidases such as VP is also related with proximal Ca^{2+} [17]. Unfortunately, no mutants of the distal Ca^{2+} binding site could be thermally characterized for comparison due to greatly lowered activity as reported [16].

Two structural calcium ions are important for maintaining the integrity of the heme environment of ligninolytic peroxidases. During thermal inactivation of LiP and MnP, only the more weakly-bound distal Ca^{2+} is thought to dissociate [17–19]. Both calcium ions were removed during alkaline treatment of LiP [17]. However, it seems that the role of Ca^{2+} in other peroxidases may be different from that in the high-redox-potential peroxidases LiP, MnP, and VP. When two calcium ions were completely removed from horseradish and peanut peroxidases, the enzymes were still 40% and 50% active, respectively [25–27]. In contrast, even when only one Ca^{2+} was released from LiP and MnP [16–20], the enzymes almost completely lost activities. In the case of VP, D48A and D187A roughly contain one mol Ca^{2+}/mol protein, and both mutations led to nearly complete loss of activities. The result of D48A is similar to that of D47A of MnP, and the mutant containing distal Ca^{2+} only was obtained for the first time [16]. S170A has higher Ca^{2+} content than D187A and D48A, but lower than WT VP, and it retained about 23% of WT VP activity. The results of S170A suggested that proximal Ca^{2+} could be still loosely bound in S170A, and some S170A proteins still contained two Ca^{2+}, whereas some had only one. Though the Ca^{2+} concentrations were not determined for other mutants, according to their activities, it might be predicted that the mutants which almost completely lost activities such as G60S, D62A, S64A, S170D, T187A, and D194A would contain only one mol Ca^{2+} (proximal or distal)/mol protein, and the Ca^{2+} content of V192T would be, just like S170A, between 1 and 2 mol Ca^{2+}/mol protein. These results demonstrated that mutation of the residues involved in two Ca^{2+} led to great change in the contents of Ca^{2+}, resulting in big effect on VP activity and other properties, and enzyme activity of VP has close relationship with the residues involved in two structural Ca^{2+} and the amount of calcium in VP. Comparison of the crystal structures of peanut peroxidase (PNP) (PDB code: 1SCH) and VP revealed that the distal calcium binding site of PNP had some unique characteristics. Distal Ca^{2+} was liganded by amino acids and one water molecule, instead of two water ligands like VP, which might explain why the rigorous conditions were required to release Ca^{2+} from PNP [16,27]. In addition, close to the calcium ligands, Asp43 and Asp50, there was a disulfide bond between Cys44 and Cys49 that formed a short loop (see Supporting Information Fig. S8) [27]. In VP, this loop was much longer and did not have a disulfide bond, and the residues corresponding to Cys44 and Cys49 of PNP are Ala49 and Ala61 of VP respectively (see Supporting Information Fig. S1, Fig. S8). This additional disulfide bond may be the reason why the heme environment and activity of PNP was not affected as significantly as VP, LiP, and MnP upon the loss of calcium. This has
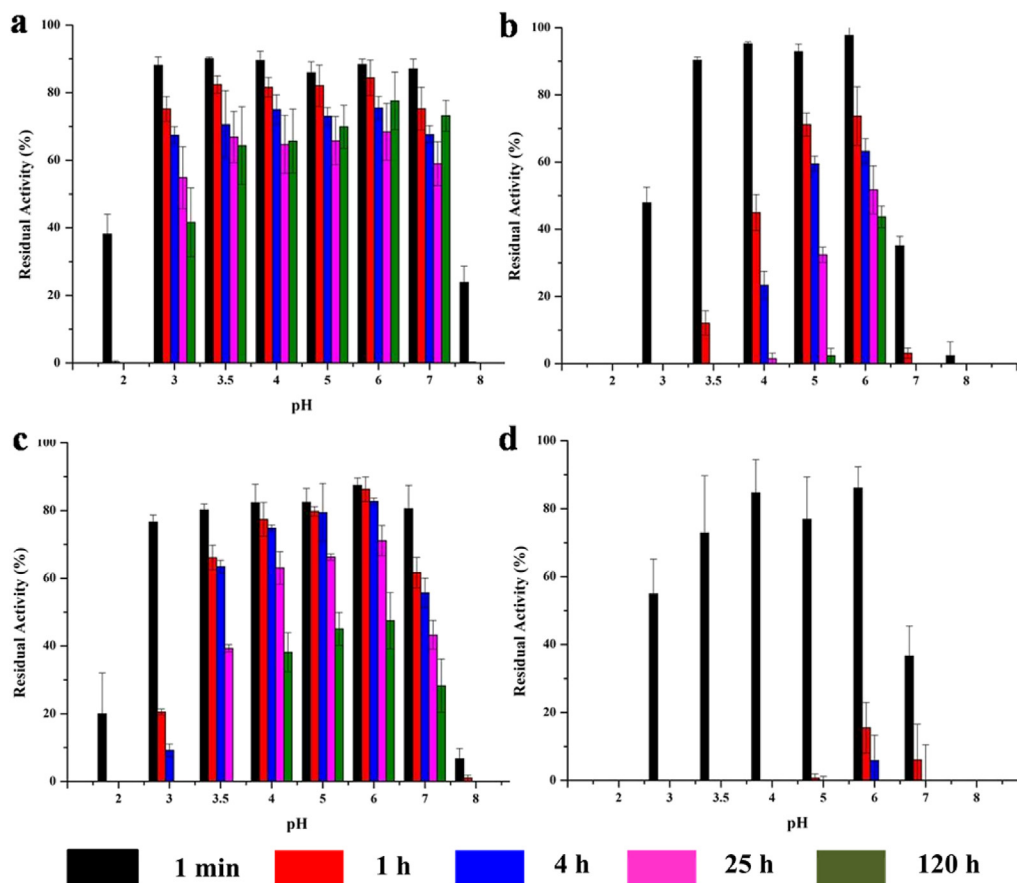
Fig. 3. pH stabilities of WT VP and three mutants. a: WT. b: S170A. c: V192T. d: S170D. The pH stability was estimated by first preincubating the purified enzymes in B & R (Britton and Robinson) buffer at different pH values (pH 2.0 to 9.0). Then the residual activities were estimated using 0.5 mM ABTS in 0.1 M sodium tartrate (pH 3.5) containing 0.1 mM H_2O_2 at 25 °C immediately after incubation at 4 °C for 1 min, 1 h, 4 h, 25 h, and 120 h respectively.
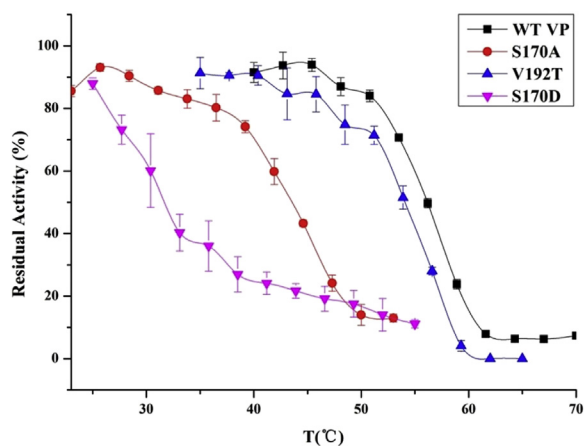
Fig. 4. Thermostabilities of wild-type VP and some mutants. Each point, including the standard deviation, was from three independent experiments. The enzymes were incubated for 10 min in a gradient temperature ranging from 40 °C to 70 °C for WT VP, 35 °C to 65 °C for V192T, 23 °C to 53 °C for S170A, and 25 °C to 55 °C for S170D respectively. After 10 min of incubation, samples were chilled on ice for 10 min and further incubated for 5 min at rt. Afterwards aliquots (50 μl) were subjected to the ABTS-based assay.

Table 3
Amount of Ca^{2+} in WT VP and three representative mutants. The amount of calcium in the VP samples was determined by inductively coupled plasma optical emission spectrometer (ICP-OES) as described in Materials and Methods.

	mol of Ca^{2+}/mol of VP	Relative activity (%)
VP	1.90 ± 0.2	100
D48A	1.1 ± 0.1	0.04
D187A	0.7 ± 0.1	0.05
S170A	1.5 ± 0.2	23.1

been proved by engineering such a disulfide bond in MnP to enhance the thermal and pH stability [20].

In comparison with WT VP, most mutants exhibited greatly reduced activities, suggesting that these residues are essential for VP. It appears that the residues, whose two mutants (S170A and V192T) retained some activities, are mainly involved in the proximal Ca^{2+} binding region. Since it is the oxygen atom of the peptide bond of Gly60 coordinating distal Ca^{2+}, mutation of Gly60 into Ser wouldn't have big effect on enzymatic activity. Unexpectedly, G60S showed significantly lower activity than WT. Close inspection of the residues around Gly60, the side chain (hydroxyl) of G60S might form a hydrogen bond with the oxygen atom of the amide bond of Leu268 according to the possible orientation of the side chain of G60S predicted by PyMOL (see Supporting Information Fig. S9). Given the fact that G60S nearly completely lost activity and it might contain only one mol Ca^{2+}/mol protein, the newly formed hydrogen bond might greatly affect the coordination environment of distal Ca^{2+} of G60S. As far as the surrounding of Val192 is concerned, its hydrophobic side chain is rightly located on the surface of the protein (see Supporting Information Fig. S10). According to
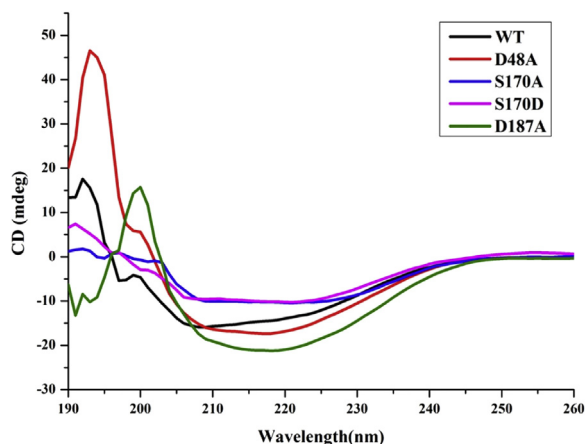
Fig. 5. Circular dichroism (CD) spectra of WT VP and several representative mutants. Far-UV CD spectra (190–260 nm) were recorded for protein samples (0.2 mg/ml) in 50 mM citrate-phosphate buffer (pH 5.5) at 25 °C.

Table 4
Secondary structure (%) estimation based on CD spectra of WT VP and mutants. Secondary-structure analyses were performed with BeStSel method [23].

	α Helix	β Strand		Turn	Others
		Antiparallel	Parallel		
WT	11.4	21.6	12	13.5	41.5
D48A	21.1	6.0	7.6	15.8	49.4
S170A	24.1	3.7	6.8	12.5	52.7
S170D	18.3	21.2	11.2	13.5	35.9
D187A	29.6	33.1	7.7	7.8	21.8

the predicted orientation for the side chain of V192T by PyMOL, it is very similar to that of Val192 (see Supporting Information Fig. S11). Thus, when it is replaced by Thr, the polar side chain (hydroxyl) of Thr may interact with water. Taking consideration into the specific activity and the possible Ca^{2+} content (between 1 and 2 mol Ca^{2+}/mol protein) of V192T, that interaction might not be so strong that coordination of proximal Ca^{2+} was not affected too much. Moreover, it's interesting to observe that there is a big difference (by two orders of magnitude) in k_{cat} between S170D and S170A. Based on all information we obtained, mutations of Ser170 into Ala and Asp had no big impact on UV–vis (see Supporting Information Figs. S3, S5), but great influence on CD (see Supporting Information Fig. S12), calcium contents and activity. S170D and S170A were further inspected by predicting the orientations of their side chains PyMOL. Based on the predicted orientation of the side chain of S170D, it could possibly form a hydrogen bond with the oxygen atom of the peptide bond of Asp194 (see Supporting Information Fig. S13). Considering that S170D might contain only one mol Ca^{2+}/mol protein, that hydrogen bond might have great impact on coordination of the proximal Ca^{2+}, and the activity of S170D would be greatly affected. In the case of S170A, though the predicted orientation of the side chain (methyl) of S170A is similar to Ser170 (see Supporting Information Fig. S14), the additional hydroxyl group of Ser could make some difference. Given the relative activity and the Ca^{2+} concentration of S170A, while it is replaced by Ala, the liganding environment of proximal Ca^{2+} was affected to some extent. It seems that the different properties (hydrophobic for methyl, hydrophilic for carboxylate) and the orientation of the side chains of Ala and Asp impacted coordination of proximal Ca^{2+} differently, and the greatly affected the liganding environment of proximal Ca^{2+} possibly led to significant influence on CD spectra, calcium contents and activities of S170A and S170D.

All in all, mutation of the residues involved in two structural Ca^{2+} influenced coordination of the proximal Ca^{2+} differently, leading to different impact on the Ca^{2+} contents of the mutants, and finally their activities and other properties such as UV–vis and CD were affected to different extent. Solving the crystal structures of some mutants such as V192A, S170D, and S170A might help to understand their different performance.

5. Conclusion

Ten mutants of the residues liganding two structural calcium ions of VP were made and fully characterized. Most mutations resulted in great loss of enzyme activity. The different impact of residues involved in two calcium ions on enzyme activity, UV–vis spectroscopy, and secondary structure was observed, and the effects of the mutants related to proximal Ca^{2+} only on enzyme activity, UV–vis spectroscopy, pH and thermal stability, and circular dichroism were presented for the first time. It was observed that the thermostability of ligninolytic peroxidases such as VP is related with proximal Ca^{2+} for the first time as well. Our results confirmed the significance of residues coordinating two structural calcium ions of ligninolytic peroxidases and close relationship between enzyme activity and Ca^{2+} concentration in protein, and would provide a guide for engineering them towards higher thermal and pH stability.

Appendix A. Supplementary data

Supplementary data related to this article can be found at http://dx.doi.org/10.1016/j.abb.2016.10.004.

References

[1] F.J. Ruiz-Dueñas, Á.T. Martínez, Microbial degradation of lignin: how a bulky recalcitrant polymer is efficiently recycled in nature and how we can take advantage of this, Microb. Biotechnol. 2 (2009) 164–177.
[2] X.-F. Tian, Z. Fang, F. Guo, Impact and prospective of fungal pre-treatment of lignocellulosic biomass for enzymatic hydrolysis, Biofpr 6 (2012) 335–350.
[3] C. Wan, Y. Li, Fungal pretreatment of lignocellulosic biomass, Biotechnol. Adv. 30 (2012) 1447–1457.
[4] A.D. Moreno, D. Ibarra, P. Alvira, E. Tomás-Pejó, M. Ballesteros, A review of biological delignification and detoxification methods for lignocellulosic bioethanol production, Crit. Rev. Biotechnol. 35 (2015) 342–354.
[5] M.J. Martínez, F.J. Ruiz-Dueñas, F. Guillén, A.T. Martínez, Purification and catalytic properties of two manganese peroxidase isoenzymes from Pleurotus eryngii, Eur. J. Biochem. 237 (1996) 424–432.
[6] T. Mester, J.A. Field, Characterization of a novel manganese peroxidase-lignin peroxidase hybrid isozyme produced by Bjerkandera species strain BOS55 in the absence of manganese, J. Biol. Chem. 273 (1998) 15412–15417.
[7] M. Pérez-Boada, W.A. Doyle, F.J. Ruiz-Dueñas, M.J. Martínez, A.T. Martínez, A.T. Smith, Expression of Pleurotus eryngii versatile peroxidase in Escherichia coli and optimisation of in vitro folding, Enzyme Microb. Technol. 30 (2002) 518–524.
[8] X. Bao, A. Liu, X. Lu, J.-J. Li, Direct overexpression, characterization and H_2O_2 stability study of active Pleurotus eryngii versatile peroxidase in Escherichia coli, Biotechnol. Lett. 34 (2012) 1537–1543.
[9] F.J. Ruiz-Dueñas, M. Morales, M. Pérez-Boada, T. Choinowski, M.J. Martínez, K. Piontek, A.T. Martínez, Manganese oxidation site in Pleurotus eryngii versatile peroxidase: a site-directed mutagenesis, kinetic, and crystallographic study, Biochemistry 46 (2007) 66–77.
[10] F.J. Ruiz-Dueñas, M. Morales, M.J. Mate, A. Romero, M.J. Martínez, A.T. Smith, A.T. Martínez, Site-directed mutagenesis of the catalytic tryptophan environment in Pleurotus eryngii versatile peroxidase, Biochemistry 47 (2008) 1685–1689.
[11] E. Garcia-Ruiz, D. Gonzalez-Perez, F.J. Ruiz-Dueñas, Á.T. Martínez, M. Alcalde, Directed evolution of a temperature-, peroxide- and alkaline pH tolerant versatile peroxidase, Biochem. J. 441 (2012) 487–498.

[12] X. Bao, X. Huang, X. Lu, J.-J. Li, Improvement of hydrogen peroxide stability of *Pleurotus eryngii* versatile ligninolytic peroxidase by rational protein engineering, Enzyme Microb. Technol. 54 (2014) 51—58.

[13] V. Sáez-Jiménez, S. Acebes, V. Guallar, A.T. Martínez, F.J. Ruiz-Dueñas, Improving the oxidative stability of a high redox potential fungal peroxidase by rational design, PLoS One 10 (2015) e0124750.

[14] D. Gonzalez-Perez, E. Garcia-Ruiz, F.J. Ruiz-Dueñas, A.T. Martinez, M. Alcalde, Structural determinants of oxidative stabilization in an evolved versatile peroxidase, ACS Catal. 4 (2014) 3891—3901.

[15] M. Pérez-Boada, F.J. Ruiz-Dueñas, R. Pogni, R. Basosi, T. Choinowski, M.J. Martínez, K. Piontek, Á.T. Martínez, Versatile peroxidase oxidation of high potential aromatic compounds: site-directed mutagenesis, spectroscopic and crystallographic investigation of three long-range electron transfer pathways, J. Mol. Biol. 345 (2005) 385—402.

[16] G.R.J. Sutherland, L.S. Zapanta, M. Tien, S.D. Aust, Role of calcium in maintaining the heme environment of manganese peroxidase, Biochemistry 36 (1997) 3654—3662.

[17] S.J. George, M. Kvaratskhelia, M.J. Dilworth, R.N.F. Thorneley, Reversible alkaline inactivation of lignin peroxidase involves the release of both the distal and proximal site calcium ions and bishistidine co-ordination of the haem, Biochem. J. 344 (1999) 237—244.

[18] G.R.J. Sutherland, S.D. Aust, The effects of calcium on the thermal stability and activity of manganese peroxidase, Arch. Biochem. Biophys. 332 (1996) 128—134.

[19] G. Nie, S.D. Aust, Effect of calcium on the reversible thermal inactivation of lignin peroxidase, Arch. Biochem. Biophys. 337 (1997) 225—231.

[20] N.S. Reading, S.D. Aust, Engineering a disulfide bond in recombinant manganese peroxidase results in increased thermostability, Biotechnol. Prog. 16 (2000) 326—333.

[21] J. Sambrook, E.F. Fritsch, T. Maniatis, Molecular Cloning: a Laboratory Manual, Cold Spring Harbor, Cold Spring Harbor Laboratory Press, 1989.

[22] S.J. Lin, E. Yoshimura, H. Sakai, T. Wakagi, H. Matsuzawa, Weakly bound calcium ions involved in the thermostability of aqualysin I, a heat-stable subtilisin-type protease of *Thermus aquaticus* YT-1, Biochim. Biophys. Acta 1433 (1999) 132—138.

[23] A. Micsonai, F. Wien, L. Kernya, Y.-H. Lee, Y. Goto, M. Réfrégiers, J. Kardos, Accurate secondary structure prediction and fold recognition for circular dichroism spectroscopy, Proc. Natl. Acad. Sci. U. S. A. 112 (2015) E3095—E3103.

[24] J. Verdín, R. Pogni, A. Baeza, M.C. Baratto, R. Basosi, R. Vázquez-Duhalt, Mechanism of versatile peroxidase inactivation by Ca^{2+} depletion, Biophys. Chem. 121 (2006) 163—170.

[25] Y. Shiro, M. Kurono, I. Morishima, Presence of endogenous calcium ion and its functional and structural regulation in horseradish peroxidase, J. Biol. Chem. 261 (1986) 9382—9390.

[26] C. Hu, D. Lee, R.N. Chibbar, R.B. van Huystee, Ca^{2+} and peroxidase derived from cultured peanut cells, Physiol. Plant 70 (1987) 99—102.

[27] D.J. Schuller, N. Ban, R.B. van Huystee, A. McPherson, T.L. Poulos, The crystal structure of peanut peroxidase,, Structure 4 (1996) 311—321.